JCAMEH

Vol. 49, No. 2, December 2018, pp 282-291
DOI: 10.22059/jcamech.2018.268899.338

Behavioral Optimization of Pseudo-Neutral Hole in Hyperelastic Membranes Using Functionally graded Cables

Reza Noroozi ,Ali Asghar Atai *

Department of Mechanical Engineering, University of Tehran, Tehran, Iran

ARTICLE INFO

Article history:
Received: 4 November 2018
Accepted: 21 November 2018

Keywords:
Hyperelastic Membrane
Neutral Hole
Optimization
Genetic Algorithm
Functional Graded Cable

ABSTRACT

Structures consisting of cables and membranes have been of interest to engineers due to their higher ratio of strength to weight and lower cost compared to other structures. One of the challenges in such structures is presence of holes in membranes, which leads to non-uniform stress and strain distributions, even under uniform far-field deformations. One of the approaches suggested for controlling this non-uniformity is reinforcing the hole edge using a cable, such that stretch changes near the hole are minimized compared to that of the far field in the membrane. In this study, considering an optimization problem, it is illustrated that for different geometries and stretch ratios in a biaxial loading of the membrane, a suitable cable of varying stiffness can be chosen such that stretch non-uniformity in the membrane is minimum, thus presenting a state of a pseudo-neutral hole in the membrane. The presented form of parametric functionally graded cable and the optimization problem solved for a couple of hole shapes show that the cable can induce a state of close to uniform stretch distribution for certain values of far field stretch ratios, it also proves effective for a range of such a ratio. Relative non-uniformity indices as low as 2 percent are achieved from optimization.

1. Introduction

Hyperelastic materials are those that show an elastic behavior for a large range of strains. In general, the behavior of these materials is nonlinear, and there are several constitutive models for them [1]. Membrane structures' history date back to the late 19^{th} century, when they were used for circus tents as well as in cable structures of small bridges. Structures consisting of membranes and cables have been of interest to engineers due to their high strength to weight ratios, easy transportation, and low cost as well as a long span coverage for a lower cost in comparison with other structures. Since these structures are normally under tension in the plane of the membrane, they are not exposed to bending and buckling like other engineering structures. Thus, they are superior to others [2]. Due to the non-linearity of geometry and material behavior, designing and analysis of these structures involve difficulties and complications. Today, analysis of membranes has gained more important because of its wide applications in biomechanics. For example, in investigating human skin behavior against stresses applied on the skin, plastic surgery, and studying the effect of machines and devices that are in contact with the skin, the skin is modeled as a hyperelastic membrane[3].

* Corresponding Author. Tel.: +98 61119951; Fax: +98 21 88013029
Email Address: aataee@ut.ac.ir

Utilizing membranes as loading-carrying structures have led to various challenges. One of these challenges is the presence of access holes and cutouts in membranes, which results in a significant change in stress distributions compared to that of the hole-free membrane. In some applications, there have to be hole present in the membrane such as Ultra-precision products which contain a micro-hole array [4] and for tents and roof structures, holes are considered in the membrane in order to attach it to the supporting poles and columns [5]. Usually, the presence of a hole causes a concentration of stress on the hole-edge, which could result in failures, or it induces regions of low-tensions or wrinkles, which could lead to bumps and potholes upon addition of rain and snow loads in roof structures. One of the solutions suggested to remedy this issue, is the hole-edge reinforcement using a cable such that stretch in the hole is equal to the stretch in the hole-free membrane at that location. Such a hole is called a neutral hole, i.e., a hole that is actually present, but it is reinforced in such a way that the membrane surrounding it is not affected by the presence of the hole. Because of the importance and elegance of this subject, there are numerous researches on investigating the effect of holes in plates and membranes, and how they can be neutralized. Gunwant and Singh investigated stress concentration and displacement within the plate for an elliptical hole in a sheet for different elliptic parameters, using the finite element method [6]. Tish et al. carried out topological design cable-net structure by using Robotic additive manufacturing and considering a functionally graded cable-net [7]. Chen, stretching a large plate in the far field, calculated an optimal shape as well as an optimal number of holes for a plate such that its stress distribution becomes uniform[8]. Saha and Ghuku investigated stress and strain distribution in a leaf spring with a circular hole [9]. Budiansky et al. presented an analytical solution for a neutral hole in a composite sheet comprised of two linear elastic materials with different Young's moduli. Several engineering solutions have been proposed to remove the non-homogeneity in stress and strain distributions. Savin showed that stress concentration could be reduced through attaching a soft ring on the inside of the [10]. Mansfield et al. created holes with different shapes in a sheet comprised of a linear elastic material and demonstrated that they could be considered as sheets without holes through reinforcing the holes [11]. Budney and Bellow applied a load on a parabolic hole in a photoelasticity test and found that a uniform stress distribution could be produced in the object through reinforcing the hole with cables of different materials [12]. Carroll et al. proposed an optimal form of cable reinforcement for a linear elastic plate with a central circular hole [13]. Atai obtained an analytical solution for reinforcing circular and elliptical holes in hyperelastic membranes under biaxial far field stretches and illustrated that, in order to achieve a completely neutral elliptic hole, there has to be a relationship between stretch ratios and geometry of the ellipse [14].

In these researches, the shape of the hole was mostly circular, and the neutrality was investigated for a specific uniaxial or biaxial stretch ratio. In this work, we present a methodology for a hole of general shape in the membrane, and by considering a parametric functionally graded cable as the reinforcement, we try to get a pseudo-neutral hole for not a specific, but a range of biaxial stretch ratios. Therefore, an optimization problem is formulated and solved. The results show that the methodology is capable of handling holes of different shapes. Moreover, considering a relatively simple parametric grading function for the cable, the optimized grading offers a pseudo-neutral hole for a range of stretch ratios effectively

2. Methodology

Fig. 1 shows a membrane with a hole, under the action of general biaxial far field stretches with η_1 and η_2 in horizontal and vertical directions, respectively. The figure also shows a differential element of the membrane in reference and deformed configuration, with principal strain directions shown by dashed lines. If λ_i , $\mathbf{u}_i$, and $\mathbf{v}_i$ (i=1, 2) are the principal stretches, and principal directions in reference and deformed configuration respectively, then the deformation gradient **F** is given by [15]

$$\mathrm{F} = \lambda_1 \mathrm{v}_1 \otimes \mathrm{u}_1 + \lambda_2 \mathrm{v}_2 \otimes \mathrm{u}_2 \tag{1}$$

Where $\otimes$ denotes the tensor product of vectors. If $w(\lambda_1, \lambda_2)$ is the strain energy function for the membrane material, then the first Piola-Kirchoff stress is expressed as [15]

$$\mathrm{T} = w_1 \mathrm{v}_1 \otimes \mathrm{u}_1 + w_2 \mathrm{v}_2 \otimes \mathrm{u}_2 \tag{2}$$

where $w_i = \partial w / \partial \lambda_i$. By defining the in-plane stretch tensor invariants as $I = \lambda_1 + \lambda_2$ and $J = \lambda_1 \lambda_2$, w_1 and w_2 can be represented by

$$w_1 = W_I + \lambda_2 W_J \tag{3}$$

where W_I and W_J are derivatives of strain energy function with respect to I and J respectively. Therefore, Eq. (2) can be rewritten in the following form

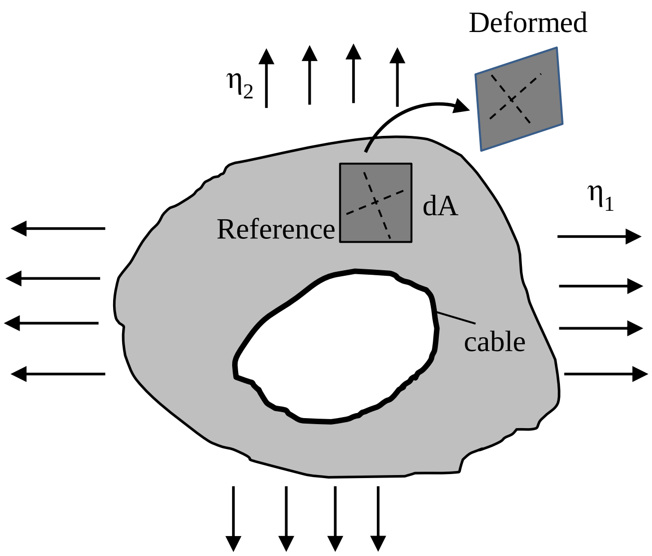

Fig. 1 Membrane with a cable reinforced hole, under far field uniform biaxial loading

$$T = (W_I + \lambda_2 W_J)v_1 \otimes u_1 + (W_I + \lambda_1 W_J)v_2 \otimes u_2 \quad (4)$$

Fig. 2 shows the hole boundary and the membrane surrounding it. From continuum mechanics, the equilibrium equation at each point of the membrane in absence of body forces is

$$div\,(T) = 0 \quad in \quad \Omega \tag{5}$$

and the hole boundary condition is [14].

$$Tv = f' \quad on \quad P \tag{6}$$

Where v is the unit outward normal to the hole boundary (Fig. 2), and $f = f(s)\tau$ is the force per unit arclength s of the cable along the unit tangent τ to the cable. It should be noted that since the equilibrium equation (5) is going to be formulated in terms of displacement, the points on the outer boundary of the membrane have a known displacement because of the far field stretch, and therefore, taking these displacements as known, no boundary condition is needed there.

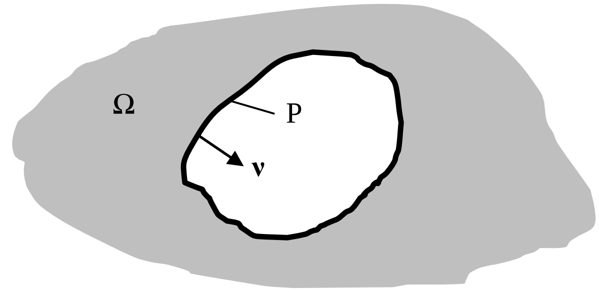

Fig. 2: Membrane and cable reinforced hole boundary

In general, eq. (5) Cannot be solved analytically, nut rather numerically. Therefore, region Ω is discretized by grid lines and this equation is approximated at the grid points, to form a set of nonlinear equations in terms of the unknown grid point displacements. Fig. 3 shows the discretized region surrounding a general grid point (i,j).

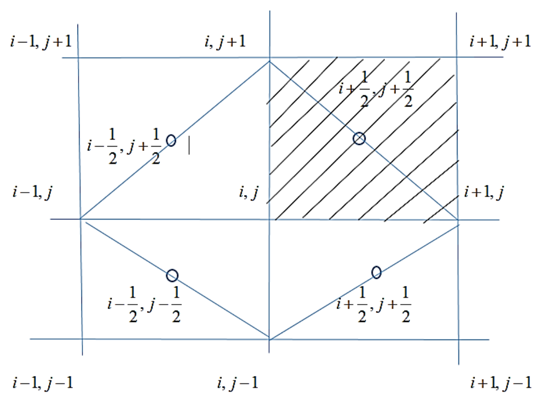

Fig. 3 discretization of the membrane

In order to calculate the deformation gradient and divergence of Piola stress for this discretization, the Green theorem, which relates the area integral of derivative of a quantity to its line integral, is used as follows

$$\iint_{\Omega} \Phi_{,\alpha}\, da = e_{\alpha\beta} \oint_{\partial\Omega} \Phi\, dx_{\beta} \tag{7}$$

where $\Phi(x)$ is a membrane field quantity, and $e_{\alpha\beta}$ is unit alternator (e_{12}=-e_{21}=1, e_{11}=e_{22}=0).

If $\mathbf{x}^{i,j}$ and $\mathbf{y}^{i,j}$ are the position vectors of the grid point (i,j) in reference and deformed configuration respectively, using eq.(7) along with the mean value theorem for the hatched region in Fig. 3 gives the deformation gradient for the center of this region (shown by a circle in this figure) as follows [15]:

$$F_{k\alpha}^{i+1/2,j+1/2} = (2A^{i+1/2,j+1/2})e_{\alpha\beta} \\ [(x_\beta^{i,j+1} - x_\beta^{i+1,j})(y_k^{i+1,j+1} - y_k^{i,j}) - \\ (x_\beta^{i+1,j+1} - x_\beta^{i,j})(y_k^{i,j+1} - y_k^{i+1,j})] \tag{8}$$

where $A^{i+1/2,j+1/2}$ is the area of hatched region approximated by

$$A^{i+1/2,j+1/2} = \frac{1}{2}[(x_2^{i,j+1} - x_2^{i+1,j})(x_1^{i+1,j+1} - x_1^{i,j}) \\ -(x_1^{i,j+1} - x_1^{i+1,j})(x_2^{i+1,j+1} - x_2^{i,j})] \tag{9}$$

From this, the principal stretches and directions, and the Piola stress at the center of each region can be calculated. Using the Green's theorem (7) again, and taking the integration on the blue line in Fig. 3, which connects the centers of regions surrounding the grid point (i,j), the equilibrium equation (5) in discretized form is given by

$$P_k^{i,j} = 2A^{i,j}(T_{k\alpha,\alpha}) = \\ e_{\alpha\beta}[T_{k\alpha}^{i+1/2,j+1/2}(x_\beta^{i,j+1} - x_\beta^{i+1,j}) \\ +T_{k\alpha}^{i-1/2,j+1/2}(x_\beta^{i-1,j} - x_\beta^{i,j+1}) + \\ T_{k\alpha}^{i-1/2,j-1/2}(x_\beta^{i,j-1} - x_\beta^{i-1,j}) \\ +T_{k\alpha}^{i+1/2,j-1/2}(x_\beta^{i+1,j} - x_\beta^{i,j-1}) \tag{10}$$

where $A^{i,j}$ is half of the area inside the blue line, given by

$$A^{i,j} = \frac{1}{2}[(x_2^{i-1,j} - x_2^{i+1,j})(x_1^{i,j+1} - x_1^{i,j-1}) \\ -(x_1^{i-1,j} - x_1^{i+1,j})(x_2^{i,j+1} - x_2^{i,j-1})] \tag{11}$$

The discretized set of equilibrium equations along with the boundary conditions are nonlinear in terms of the unknowns $\mathbf{y}^{i,j}$. Atai and Steigmann used Dynamic Relaxation method to solve these equations in an iterative way[14], and the same method is adopted here. The reader can refer to these references for details of implementation of the method. Considering a grading function for the cable ($f(s)$ or $f(\theta)$, where θ is the angle parameter corresponding to the cable arc length s), and far-field stretches with η_1 and η_2, the equilibrium state of the membrane is obtained and the distribution of the principal stretches can be compared to those in the far field to quantify the effectiveness of cable reinforcement for a neutral hole.

In this work a very simple trigonometric series with finite number of terms is considered for the cable grading function as follows

$$f = a_0 + \sum_{n=1}^{N} a_n \operatorname{Sin}(n\theta) + b_n \operatorname{Cos}(n\theta) \tag{12}$$

The justification for this choice is just the necessary periodicity of the grading around the cable, and it will be shown in the next section that this simple model can handle different hole shapes and stretch ratios in order for the hole to become pseudo-neutral. The coefficients a_i and b_i in this model are considered as the design variables of the optimization problem. As a measure of the non-uniformity of the stretch distribution in the cable-reinforced membrane, the following quantity is defined, which is to be minimized as the objective function of the problem

$$NU = \sum_{i=1}^{M} (\eta_1 - \lambda_{1i})^2 + (\eta_2 - \lambda_{2i})^2 \tag{13}$$

Where M is the number of regions in the discretized membrane. In this work, the case of pseudo-neutrality is also examined for a range of far-field stretch ratios. To implement that, the far field stretches are considered at some discrete values (η_{1j}, η_{2j}) j=1,..,L in the range, and the objective function (13) is extended as follows

$$NUR = \sum_{j=1}^{L}\sum_{i=1}^{M} (\eta_{1j} - \lambda_{1ij})^2 + (\eta_{2j} - \lambda_{2ij})^2 \tag{14}$$

As for the optimization method, it is noted that the stretch distribution used in defining the objective functions (13)(13) and (14) is not an explicit mathematical function of the design variables, and the nature of design variables is such that they might take any real value, as long as $f(\theta)$ is a non-negative number. These facts mean that the design space is very large, and non-mathematical direct methods have to be used for optimization. It is also expected that the problem might have several optimum points at different places in design space. This calls for an evolutionary multi-agent method. The authors have used the well-established genetic algorithm for this purpose without running into any difficulties to call for usage of another method. Therefore, it seems unnecessary here to present a discussion on the method of optimization.

3. Results

For simplicity, the stretch ratio in far from on the membrane η_2/η_1 is represented as ξ. Also, the stretch ratio in the membrane λ_2/λ_1 is presented as κ.

As a first example, the case of an elliptic hole (Fig. 4) is examined. Atai and Steigmann [16] proved that for this case, if the far field stretch is related to the hole dimensions as follows

$$\frac{a}{b}=\left(\frac{\eta_2(W_I+\eta_2 W_J)}{\eta_1(W_I+\eta_1 W_J)}\right)^{1/2} \tag{15}$$

then the hole is exactly neutral, provided that the cable is graded as

$$f=b(W_I+\lambda_2 W_J)\left(\frac{\lambda_2^{\,2}}{\lambda_1^{\,2}}\frac{b^2}{a^2}\mathrm{Cos}^2\,\theta+\mathrm{Sin}^2\,\theta\right) \tag{16}$$

This case is considered here for examination of optimization methodology, although the grading function (12) is significantly different in form, compared to the one considered in (16). For the numerical implementation, the hole dimensions are considered to be *a*=5 and *b*=4. The hyperelastic material is considered to be Varga, for which [19]

$$W_I=2\mu \tag{17}$$

$$W_J=-2\mu J^{-2}$$

And a value 1 is considered for the shear modulus μ for simplicity. Using these choices, the stretch ratio from the condition (18) is calculated to be $\xi=\eta_2/\eta_1=1.71$. Also because of symmetry, only a quarter of the domain is considered for cable grading and membrane analysis (Fig. 5)

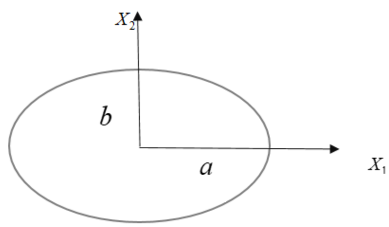

Fig. 3: Geometry of the elliptic hole

For this case, the grading function (13) is considered to include just the constant term a_0, along with sinusoidal terms in the series up to N=5, as a trial, and to keep the list of design variables short. Table 1 presents values of design variables after optimization. It is seen that the coefficients of the first few terms are of more significant, and that also justifies why very few terms are considered in the grading function.

Table 1: Optimization Results Obtained for the Elliptical Hole with Stretch Ratio of ξ=1.71

Coefficients	Values
a_0	5.609
a_1	6.46050
a_2	4.58×10^{-4}
a_3	1.614×10^{-3}
a_4	9.0322×10^{-4}
a_5	1.04225×10^{-1}

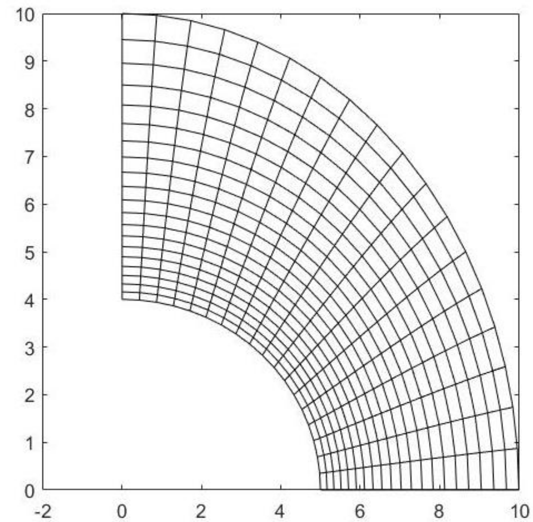

Fig. 5. Membrane with an elliptic hole: quarter model and grid lines for analysis

As for post-solution analyses, first, the cable grading is considered. Fig. 6 compares the optimized cable grading and the analytical one given by (16) along the cable. It is seen that they differ by as much as %15, which is anticipated because of different grading functions, and the few numbers of terms in the series considered here.

Now, the effectiveness of optimized cable is investigated. Fig. 7 shows the distribution of stretch ratio $\kappa=\lambda_2/\lambda_1$ for the membrane points along the x_1 axis (Fig. 4), for the membrane with no cable reinforcement. It indicates that the strain distribution in the membrane is highly non-uniform.

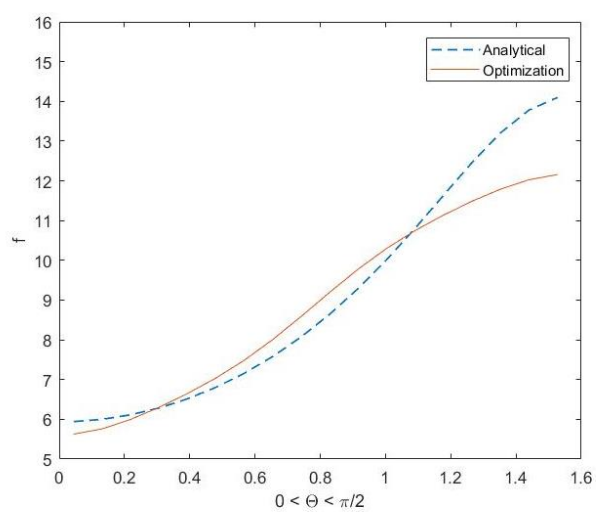

Fig. 6: Comparison of cable grading for an analytical and optimized solution for the elliptic hole with ξ=1.71

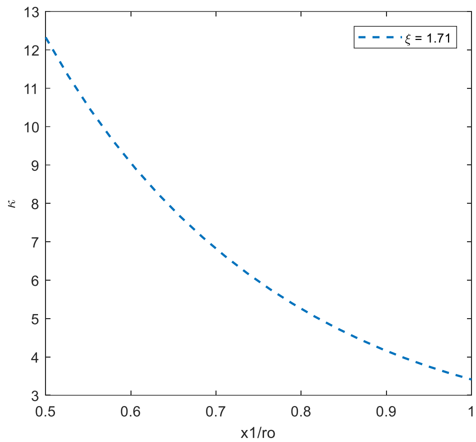

Fig. 7: distribution κ for the membrane with unreinforced elliptic hole for ξ=1.71

This non-uniformity is more pronounced, by looking at the distribution of each of principal stretches in the domain, which are presented in Figs. 8 and 9.

Now the effect of optimized cable is considered, and Figs. 10, 11 and 12 are the counterparts of Figs. 7, 8 and 9 for the reinforced membrane. It is clear that although the optimized grading function does not appear to be similar to the exact one, but it has done the job in providing a very close to uniformly loaded membrane.

Now, let's assume a hyperelastic Neo-Hookean membrane with the same elliptical hole which undergoes a far-field biaxial stretch ration in the range $1<\xi<2$. From the constitutive law for this material we have [17].

$$W_I = \mu I \qquad (18)$$
$$W_J = -\mu(1+J^{-3})$$

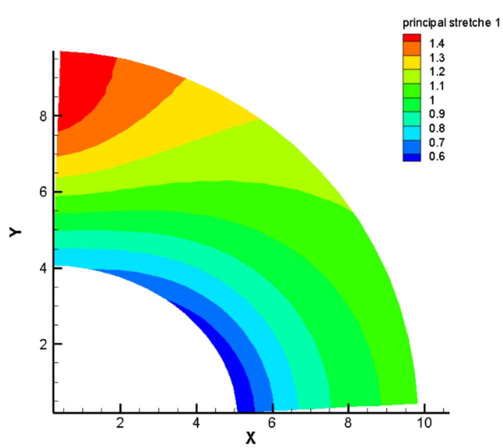

Fig. 8: Distribution of λ_1 for the membrane with unreinforced elliptic hole for ξ=1.71

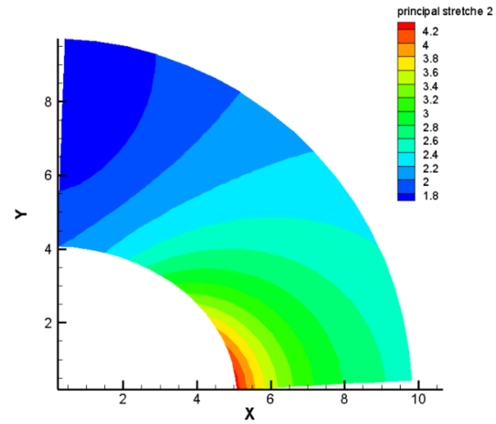

Fig. 9: Distribution of λ_2 for the membrane with unreinforced elliptic hole for ξ=1.71

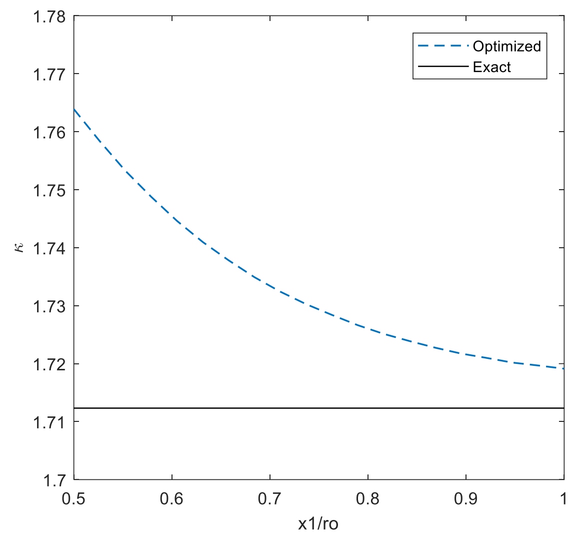

Fig. 10: κ distribution for the membrane with unreinforced elliptic hole for ξ=1.71: exact vs. optimized

Again, considering the same grading function as in the first example, and considering L=3 specific values for the stretch ration in this range, namely ξ=1, ξ=1.71, and ξ=2, the objective function (14) is optimized. Table 2 presents the optimized grading coefficients. Again, it is seen that only the first few parameters are significant.

Fig. 13 shows the principal stretch ratio for membrane points on the x_1 axis, for each of the selected far field stretch ratios. It is seen that although there is less uniformity compared to that of single stretch ratio value, but overall, the reinforcement has helped to get a close-to-uniform stress state for the considered range of ξ. This is better seen while considering distributions for ξ values other than the initially three selected numbers. Fig.

14 shows the result and confirms the close-to-uniform stress state for the whole range.

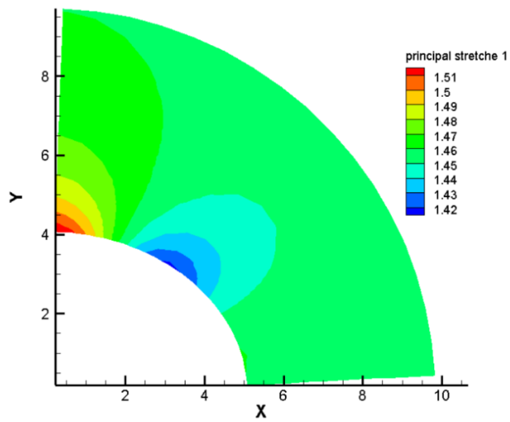

Fig. 11: Distribution of λ_1 for membrane with the optimally reinforced elliptic hole for ξ=1.71

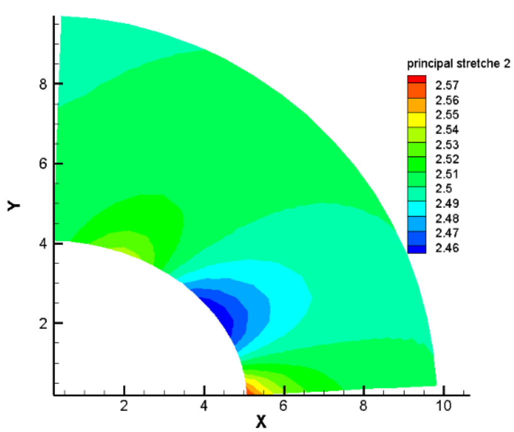

Fig. 12: Distribution of λ_2 for membrane with the optimally reinforced elliptic hole for ξ=1.71

Table 2 Results of Optimization for the Elliptical Hole

Coefficients	Values
a_0	8.2431
a_1	3.8109
a_2	0.126
a_3	8.247×10^{-4}
a_4	1.62×10^{-3}
a_5	2.07×10^{-3}

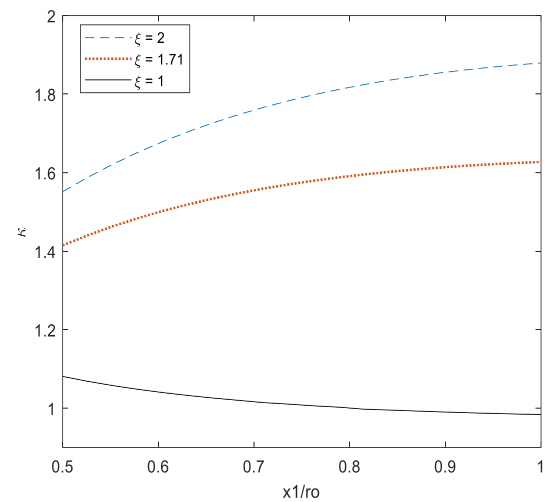

Fig. 13: Distribution of κ for Optimization Results

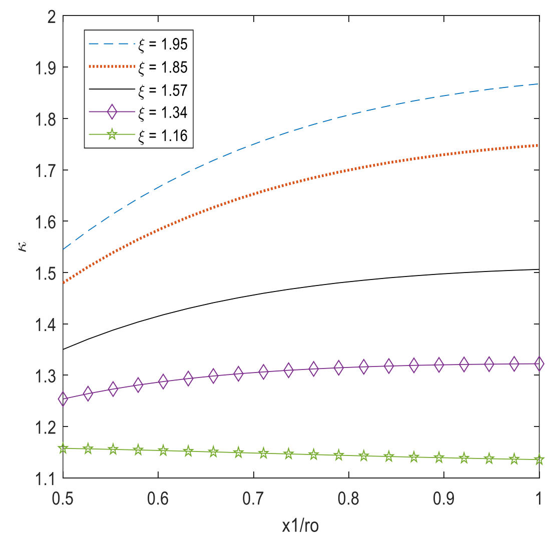

Fig. 14: Distribution of κ for the range $1<\xi<2$

As the last example, the case of a pseudo-square hole is considered. The hole boundary is obtained as a special case of the general class of closed curves resulting from the following expression [18]:

$$\frac{(x^2+y^2)}{4}+\sum_{n=-\infty}^{n=\infty}\left[a_n\,\mathrm{Re}(z^n)+b_n\,\mathrm{Im}(z^n)\right]=0 \tag{19}$$

where z=x+i y is the complex number. It can be verified that for the values of $a_0=-\dfrac{1}{4}$ and $a_4=\dfrac{5}{100}$, (all other coefficients being zero), it gives the shape of a pseudo-square boundary shown in Fig. 15.

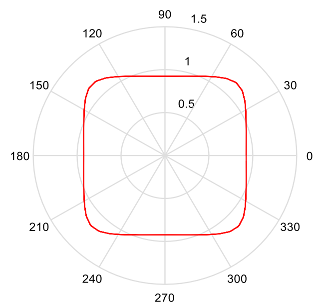

Fig. 15: Pseudo-Square Boundary

In this case, too, it is possible to consider a quarter of the domain to reduce computation time. The same grading function and stretch ratio range, and selected values for ξ in the range, as that of the elliptic hole case are considered here, and the material is Neo-Hookean.

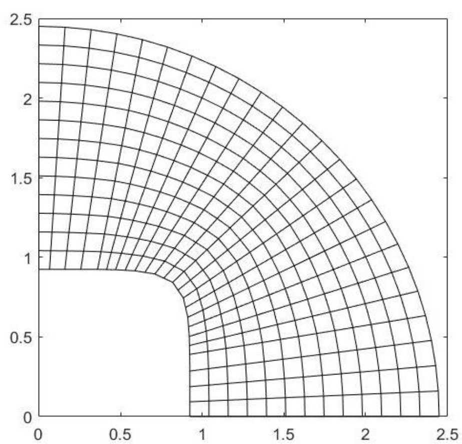

Fig. 16 A membrane with a Pseudo-Square Hole, Non-deformed Case

To get a better idea of cable effect, first the distribution of κ in the non-reinforced membrane for the case of $\xi = 1.71$ is shown in Fig. 17, illustrating non-uniformity.

Table 3 presents the optimized design variables for this example, once again showing the significance of the first few parameters.

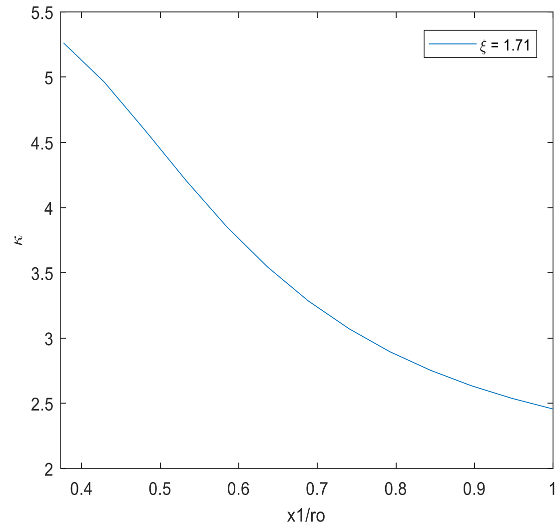

Fig. 17: Distribution of Stretch Ratio, without Reinforcement Cable for $\xi = 1.71$

Table 3 Results of Optimization for the Pseudo-Square Hole for three Stretch Ratios

Coefficients	Values
a_0	1.3674
a_1	2.383
a_2	0
a_3	1.23979×10^{-4}
a_4	3.9653×10^{-5}
a_5	0

Fig. 18 shows the κ distribution on the horizontal axis for the three selected values of ξ. The more pronounced non-uniformity close to the hole edge could possibly attributed to the almost straight edge of the pseudo-square at that region. However, for the most part of the domain, an almost uniform distribution is observed.

This trend is also observed for other values of ξ in the range, shown in Fig. 19, from which it can be concluded that the optimized cable works for a range of stretch effectively.

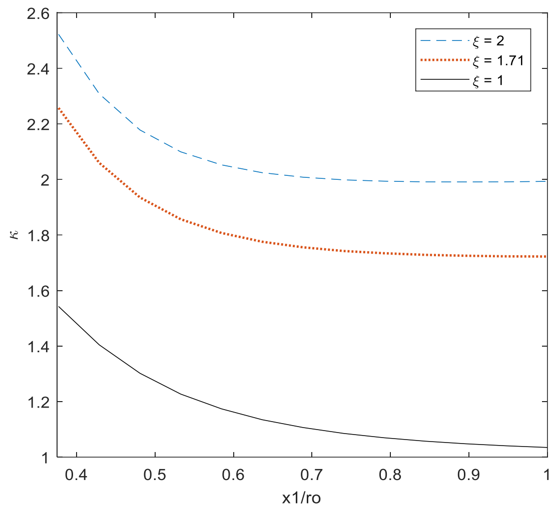

Fig. 18: Distribution of κ for Results of the Optimization

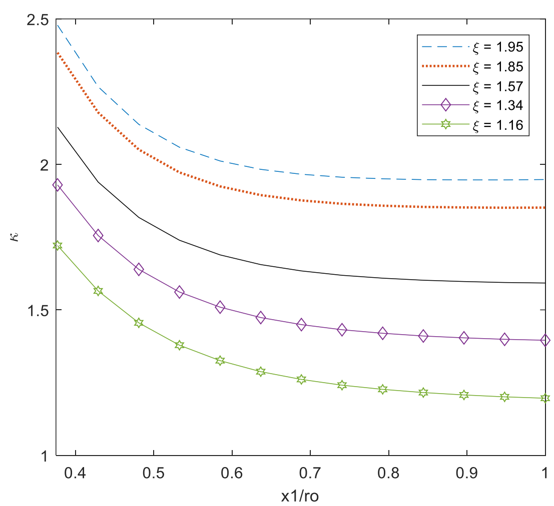

Fig. 19: Distribution of κ for Different Values of ξ for pseudo-square hole

4. Conclusion

In this study, the problem of functionally graded cable-reinforcement of a membrane with a hole under the action of a range of far-field stretch ratios was formulated as an optimization problem. The grading function for the cable was considered as a parametric trigonometric series with finite number of terms, and picking a set of values for the parameters as the design variables, the discretized form of the reinforced membrane equilibrium equations was solved numerically, in order to get the stretch distribution in it, and by comparing this distribution with that of the far field, the objective function of the problem was defined. By considering several examples, it was shown that:

- The method is capable of handling holes of different shapes
- Only a few terms of the grading function are needed in most cases to achieve a psedu-neutral hole case
- The method works very well for a specific far field stretch ratio
- The method also proves effective when a range of far-field stretch ratios are considered, although the non-uniformity close to the whole edge is more pronounced

As a future work, the cases of functionally graded membranes, or membranes having multiple holes can be considered.

References

[1] J. E. Mark, B. Erman, M. Roland, 2013, *The science and technology of rubber*, Academic press,

[2] B. H. Topping, P. Iványi, 2008, *Computer aided design of cable membrane structures*, Saxe-Coburg Publications,

[3] S. L. Evans, On the implementation of a wrinkling, hyperelastic membrane model for skin and other materials, *Computer methods in biomechanics and biomedical engineering*, Vol. 12, No. 3, pp. 319-332, 2009.

[4] W.-K. Choi, S.-H. Kim, S.-G. Choi, E.-S. Lee, Quadrilateral Micro-Hole Array Machining on Invar Thin Film: Wet Etching and Electrochemical Fusion Machining, *Materials*, Vol. 11, No. 1, pp. 160, 2018.

[5] L. Gründig, E. Moncrieff, P. Singer, D. Ströbel, High-performance cutting pattern generation of architectural textile structures, in *Proceeding of*.

[6] D. Gunwant, J. Singh, Stress and displacement analysis of a rectangular plate with central elliptical hole, *Int J Eng Innov Technol*, Vol. 3, No. 3, pp. 387-392, 2013.

[7] D. Tish, W. McGee, T. Schork, G. Thün, K. Velikov, Case Studies in Topological Design and Optimization of Additively Manufactured Cable-nets, in *Proceeding of*, Elsevier, pp.

[8] N. Younis, Assembly stress for the reduction of stress concentration, *Mechanics research communications*, Vol. 33, No. 6, pp. 837-845, 2006.

[9] S. Ghuku, K. N. Saha, An experimental study on stress concentration around a hole under combined bending and stretching stress field, *Procedia Technology*, Vol. 23, pp. 20-27, 2016.

[10] B. Budiansky, J. Hutchinson, A. Evans, On neutral holes in tailored, layered sheets, *Journal of applied mechanics*, Vol. 60, No. 4, pp. 1056-1058, 1993.

[11] R. MEMORANDA, Neutral Holes in Plane Sheet: Reinforced Holes which are Elastically Equivalent to the Uncut Sheet.

[12] D. Budney, D. Bellow, On the analysis of neutral holes, *Experimental Mechanics*, Vol. 22, No. 9, pp. 348-353, 1982.

[13] E. H. Mansfield, C. J. Hanson, 1973, *Optimum reinforcement around a circular hole in a flat sheet under uniaxial tension*, HM Stationery Office,

[14] A. A. Atai, 1999, *Finite deformation of elastic curves and surfaces*,

[15] E. Haseganu, D. Steigmann, Analysis of partly wrinkled membranes by the method of dynamic relaxation, *Computational Mechanics,* Vol. 14, No. 6, pp. 596-614, 1994.

[16] A. Atai, D. Steigmann, Coupled deformations of elastic curves and surfaces, *International Journal of Solids and Structures,* Vol. 35, No. 16, pp. 1915-1952, 1998.

[17] A. C. Pipkin, The relaxed energy density for isotropic elastic membranes, *IMA journal of applied mathematics*, Vol. 36, No. 1, pp. 85-99, 1986.

[18] S. P. Timoshenko, J. M. Gere, Théorie de la stabilité élastique, *Paris: Dunod,| c1966, 2eme ed.,* 1966.